CHIN. PHYS. LETT. Vol. 37, No. 1 (2020) 015201

On the Nonlinear Growth of Multiphase Richtmyer–Meshkov Instability in Dilute Gas-Particles Flow *

Huan Zheng(郑欢)[1], Qian Chen(陈潜)[1], Baoqing Meng(孟宝清)[1],
Junsheng Zeng(曾军胜)[2], Baolin Tian(田保林)[1,2]**

[1]*Institute of Applied Physics and Computational Mathematics, Beijing 100094*
[2]*College of Engineering, Peking University, Beijing 100871*

(Received 28 September 2019)

We discuss evolutions of nonlinear features in Richtmyer–Meshkov instability (RMI), which are known as spikes and bubbles. In single-phase RMI, the nonlinear growth has been extensively studied but the relevant investigation in multiphase RMI is insufficient. Therefore, we illustrate the dynamic coupling behaviors between gas phase and particle phase and then analyze the growth of the nonlinear features theoretically. A universal model is proposed to describe the nonlinear finger (spike and bubble) growth velocity qualitatively in multiphase RMI. Both the effects of gas and particles have been taken into consideration in this model. Further, we derive the analytical expressions of the nonlinear growth model in limit cases (equilibrium flow and frozen flow). A novel compressible multiphase particle-in-cell (CMP-PIC) method is used to validate the applicability of this model. Numerical finger growth velocity matches well with our model. The present study reveals that particle volume fraction, particle density and Stokes number are the three key factors, which dominate the interphase momentum exchange and further induce the unique property of multiphase RMI.

PACS: 52.57.Fg, 52.57.−z, 47.20.−k, 52.50.Lp DOI: 10.1088/0256-307X/37/1/015201

The Richtmyer–Meshkov instability (RMI) occurs when an arbitrarily perturbed interface separating two fluids is impulsively accelerated by a shock wave.[1−3] Under shock, the involved interface becomes unstable. Small perturbations will grow to form nonlinear structures such as spikes and bubbles.[4−6] Investigating the evolution of this hydrodynamic phenomenon is important in understanding the mechanism of supernova explosions, inertial confinement fusion (ICF), etc.[7,8] Therefore, RMI has aroused the interest of researchers after introduced by Richtmyer[9] and Meshkov.[10]

Current research of RMI has mostly focused on the situation of single-phase flow. However, particles could easily affect the hydrodynamic behavior of gas.[11−16] Multiphase flow (especially gas-particle flow) involving shock waves, such as particle imaging velocimetry (PIV) technology,[17−18] explosions with reactive metal particles, was commonly seen in engineering and applications.[19−22] The RMI effects in these cases must be deeply understood. Generally, there are two special cases in gas-particle flow: equilibrium flow and frozen flow. In the equilibrium flow, particles respond to the gas motion immediately. In frozen flow, particles nearly show no response to the gas motion.[23,24] In these two special gas-particle flows, the dynamic coupling behaviors between gas phase and particle phase can be analytically illustrated.[25]

In the research of RMI, one of the primary interests and the most important problems is to predict the growth rates of the nonlinear structures, since it is a direct measurement of the mixing zone of the two fluids.[1,26] The relevant amplitude growth model in linear stage is fully understood.[12,27,28] In multiphase RMI. Ukai *et al.* applied the linear stability analysis to the governing equations and derived a theoretical model for linear multiphase RMI growth rate in dilute gas-particle flow.[12] Meng *et al.* extended this model and proposed a multiphase RMI Atwood number appropriate for both dilute gas-particle flow and dense gas-particle flow.[27] Nonlinear growth in multiphase RMI has also been investigated. Balakrishnan *et al.* developed a multiphase buoyancy-drag model for both single-mode and multi-mode interface instability.[29] With this model, they further investigated the trends of finger growth.[26] However, analytical solutions for both spikes and bubbles over all time in multiphase RMI are still unknown.

The potential flow model is one of the most effective methods in studying the nonlinear finger growth in RMI. This method was firstly introduced by Layzer in studying a vacuum bubble in RTI and then used to study bubbles in RMI.[30−32] Later, Zhang extended the potential flow model to spike with infinite density ratios and Goncharov applied this model to arbitrary density ratios.[33,34] Recently, Zhang generalized a universal finger (bubble or spike) growth model in two-dimensional RMI and RTI with all density ratios. With this model, one can collapse the main behaviors of growth rates of all fingers onto a single curve.[3] The potential flow model is useful and well developed in investigating the nonlinear stage in single-phase interface instability but has not been extended and verified in multiphase RMI. Therefore, the particular interest of this study is to introduce this research method to multiphase RMI.

*Supported by the National Natural Science Foundation of China under Grant Nos. 91852207, 11801036, 11502029, and the NSAF under Grant No. U1630247.
**Corresponding author. Email: tian_baolin@iapcm.ac.cn
© 2020 Chinese Physical Society and IOP Publishing Ltd

In this Letter, several universally used assumptions are introduced to simplify the deviation process: (1) gas and particles are both incompressible after the shock wave travels through the interface; (2) the volume fraction of particles phase is relatively small; (3) particles are homogeneously distributed; (4) the density and radius of particles are the same; and (5) particles are spherical and the drag force obeys the Stokes law.[23,24,35]

Under these conditions, the motion equations of gas phase and particle phase can be written as

$$\alpha_{\rm f}\rho_{\rm f}\frac{d\boldsymbol{u}_{\rm f}}{dt} = -\alpha_{\rm f}\nabla p - \frac{\alpha_{\rm p}\rho_{\rm p}}{\tau}\left(\boldsymbol{u}_{\rm f}-\boldsymbol{v}_{\rm p}\right), \tag{1}$$

$$\frac{d\boldsymbol{v}_{\rm p}}{dt} = -\frac{1}{\rho_{\rm p}}\nabla p + \frac{1}{\tau}\left(\boldsymbol{u}_{\rm f}-\boldsymbol{v}_{\rm p}\right) - \boldsymbol{A}_{\rm p}, \tag{2}$$

where p is the pressure of gas phase, ρ is the density, α represents the volume fraction. The subscripts p and f correspond to particle phase and gas phase, respectively; $\boldsymbol{u}_{\rm f}$ and $\boldsymbol{v}_{\rm p}$ are the average velocities of gas phase and particle phase, respectively. $\boldsymbol{A}_{\rm p}$ is the collision force, τ is a parameter referring as the response time of particles. The expression of τ is given as $\tau = m_{\rm p}/k$ with $m_{\rm p}$ being the mass of particles and k the drag term.

The collision force and gravitational acceleration term are neglected when studying multiphase RMI in dilute gas-particle flow. Combining Eq. (1) and (2), the evolution of the velocity differences between particle and gas is

$$\frac{d\left(\boldsymbol{u}_{\rm f}-\boldsymbol{v}_{\rm p}\right)}{dt} = -\left(\frac{1}{\rho_{\rm f}}-\frac{1}{\rho_{\rm p}}\right)\nabla p - \frac{1}{\tau}\left(\frac{\alpha_{\rm p}\rho_{\rm p}}{\alpha_{\rm f}\rho_{\rm f}}+1\right)\cdot\left(\boldsymbol{u}_{\rm f}-\boldsymbol{v}_{\rm p}\right). \tag{3}$$

Further, with Eq. (1) and (3), the motion equation of gas phase in gas-particle flow can be rewritten as

$$\frac{d\boldsymbol{u}_{\rm f}}{dt} = -\frac{1}{\bar{\rho}}\nabla p + \frac{d\left(\boldsymbol{u}_{\rm f}-\boldsymbol{v}_{\rm p}\right)}{dt}\frac{\alpha_{\rm p}\rho_{\rm p}}{\bar{\rho}}, \tag{4}$$

where $\bar{\rho} = \alpha_{\rm f}\rho_{\rm f}+\alpha_{\rm p}\rho_{\rm p}$ is defined as the equivalent density. In general, the velocities of particle phase and gas phase do not change synchronously due to the different response times of particles. Thus, we introduce the following relation

$$\frac{d\left(\boldsymbol{u}_{\rm f}-\boldsymbol{v}_{\rm p}\right)}{dt} = f(St)\frac{d\boldsymbol{u}_{\rm f}}{dt}. \tag{5}$$

The Stokes number is $St = \tau/(\lambda/v_{0,m}) = \tau/\tau_{\rm RMI}$, λ is the wave length of the initial perturbations, and $v_{0,m}$ is the initial growth rate of RMI. Combining with Eq. (5), the momentum equation of gas phase is

$$\frac{d\boldsymbol{u}_{\rm f}}{dt} = -\frac{1}{\bar{\rho}(1-f(St)\frac{\alpha_{\rm p}\rho_{\rm p}}{\bar{\rho}})}\nabla p. \tag{6}$$

With this equation, we can use the potential flow model to study the nonlinear finger growth in multiphase RMI.

In dilute gas-particle flow, we assume that the velocity of gas phase $\boldsymbol{u}_{\rm f}$ can be replaced by a potential function φ, as $\boldsymbol{u}_{\rm f} = \nabla\varphi$. Considering two irrotational, incompressible, inviscid fluids consisting of particles in a two-dimensional (2D) geometry, we can rewrite Eq. (6) as

$$\bar{\rho}_i\Big(1-f(St_i)\frac{\alpha_{p,i}\rho_{p,i}}{\bar{\rho}_i}\Big)\nabla\Big(\Big(\frac{\partial\varphi_i}{\partial t}+\frac{u_{f,i}^2}{2}\Big)+p_i\Big) = 0, \quad i=1,2. \tag{7}$$

The subscript i denotes the variables of fluid 1 or fluid 2. The interface position is located at $y = \eta(x,t)$. The y axis is chosen in the direction of streamwise, the x axis is chosen in the direction of spanwise. With Bernoulli's equation,[3,33,34] we derive the equations for pressure balance in multiphase RMI:

$$\sum_{i=1}^{2}(-1)^i\bar{\rho}_i(1-f(St_i)\frac{\alpha_{p,i}\rho_{p,i}}{\bar{\rho}_i}) \cdot\left(\frac{\partial\varphi_i}{\partial t}+\frac{1}{2}\left[\left(\frac{\partial\varphi_i}{\partial x}\right)^2+\left(\frac{\partial\varphi_i}{\partial y}\right)^2\right]\right) = F(t). \tag{8}$$

Together with the continuous equation of gas phase,

$$\nabla^2\varphi(t,x,y) = 0, \tag{9}$$

and the continuity condition for the velocity component normal to the fluid interface,

$$\frac{\partial\eta}{\partial t}-\frac{\partial\varphi_i}{\partial x}\frac{\partial\eta}{\partial x}+\frac{\partial\varphi_i}{\partial y} = 0,\ i=1,2,\ \text{at } y=\eta, \tag{10}$$

we can obtain the governing equations of the potential flow model for finger growth in multiphase RMI.

These governing equations are consistent with the results in the literature by replacing ρ_i with $\bar{\rho}_i(1-f(St_i)\alpha_{p,i}\rho_{p,i}/\bar{\rho}_i)$.[3] Thus, the potential function in Zhang's work is adopted to investigate the nonlinear behavior in multiphase RMI.

$$\varphi_i(t,x,y) = a_i(t)\cos(kx)\mathrm{e}^{(-1)^i ky} + b_i(t)\cos(c(t)kx)\mathrm{e}^{(-1)^i c(t)ky},\ i=1,2, \tag{11}$$

where k is the wave number. The shape of a bubble or spike tip is approximated as a parabola: $z = \eta(x,t) = y_0(t)+\xi_0(t)kx^2$. Undetermined functions $a_i(t)$, $b_i(t)$, $c(t)$, $y_0(t)$ and $\xi(t)$ are all functions of equivalent Atwood number $\bar{A}$, which is defined as

$$\bar{A} = \frac{\bar{\rho}_2(1-f(St_2)\frac{\alpha_{p,2}\rho_{p,2}}{\bar{\rho}_2})-\bar{\rho}_1(1-f(St_1)\frac{\alpha_{p,1}\rho_{p,1}}{\bar{\rho}_1})}{\bar{\rho}_2(1-f(St_2)\frac{\alpha_{p,2}\rho_{p,2}}{\bar{\rho}_2})+\bar{\rho}_1(1-f(St_1)\frac{\alpha_{p,1}\rho_{p,1}}{\bar{\rho}_1})}. \tag{12}$$

It should be noted that this equivalent Atwood number still contains undetermined function $f(St)$. Because of the complexity of multiphase flow, it is difficult to give the general expressions of $f(St)$. However, we can obtain the analytical solution at the limit

states with the definitions of Stokes number.

$$\frac{d\boldsymbol{v}_\mathrm{p}}{dt} = \frac{d\boldsymbol{u}_\mathrm{f}}{dt},\ St \to 0,\ f(St) = 0,\ \text{for equilibrium flow},$$
$$\frac{d\boldsymbol{v}_\mathrm{p}}{dt} = 0,\ St \to \infty,\ f(St) = 1,\ \text{for frozen flow}. \quad (13)$$

Therefore, the corresponding expression of the equivalent Atwood number can be obtained as follows:

$$\bar{A} = \frac{\bar{\rho}_2 - \bar{\rho}_1}{\bar{\rho}_2 + \bar{\rho}_1},\ \text{for equilibrium flow}, \quad (14)$$

$$\bar{A} = \frac{\alpha_{f,2}\rho_{f,2} - \alpha_{f,1}\rho_{f,1}}{\alpha_{f,2}\rho_{f,2} + \alpha_{f,1}\rho_{f,1}},\ \text{for frozen flow}. \quad (15)$$

Up to now, we give the expression for $\bar{A}$ and then obtain the analytical expression for it at limit states (frozen flow and equilibrium flow).

Next, we derive the nonlinear finger growth model with $\bar{A}$. Similar to Zhang's work, we can reach the following equation:

$$\frac{\mathrm{d}v}{\mathrm{d}t} = -\beta k\left(v^2 - v_\mathrm{qs}^2\right), \quad (16)$$

where v is defined as $v = dy_0/dt$, v_qs is the asymptotical finger growth velocity, which is zero in RMI; β is the function of equivalent Atwood number, which is defined as

$$\beta = \frac{3}{4}\frac{(1+\bar{A})(3+\bar{A})}{\left[3+\bar{A}+\sqrt{2}(1+\bar{A})^{1/2}\right]} \cdot \frac{\left[4(3+\bar{A})+\sqrt{2}(9+\bar{A})(1+\bar{A})^{1/2}\right]}{\left[(3+\bar{A})^2+2\sqrt{2}(3-\bar{A})(1+\bar{A})^{1/2}\right]}. \quad (17)$$

We use the positive equivalent Atwood number for bubbles and the negative counterpart for spikes with the same density ratio.[3] Then, the match solution for v can be obtained by solving Eq. (16),

$$u_\mathrm{RM} = \frac{1}{1+\tau_\mathrm{RM}}. \quad (18)$$

where $u_\mathrm{RM} = v/v_0$ and $\tau_\mathrm{RM} = \beta k v_0 t$ are the dimensionless velocity and time, respectively; v_0 is the initial velocity of finger tip. In this way, a universal finger growth model (Eq. (18)), which only depends on equivalent Atwood number and initial growth velocity, is appropriate for both spikes and bubbles in multiphase RMI.

To verify the applicability of the model, numerical simulations are conducted by the compressible multiphase particle-in-cell (CMP-PIC) method.[27] A shock driven RMI on an air/SF_6 interface surrounded by particles is investigated in this work. The initial computational domain and parameters setting are presented in Fig. 1. Two different kinds of gas (air and SF_6) are separated by a sinusoidal disturbed interface:

$$\eta(y) = \eta_0 \cos\left(\frac{2\pi}{\lambda}y\right). \quad (19)$$

The amplitude of the initial perturbations is $\eta_0 = 0.5\,\mathrm{mm}$ and the wave length is $\lambda = 10\,\mathrm{mm}$. Particles are uniformly distributed in the grey area. The single-mode RMI will be induced in this gas-particle flow. The whole computational domain is set as $(L_x, L_y) = (0.12\,\mathrm{m},\ 0.01\,\mathrm{m})$. The shock, the particle cloud front and the perturbed species interface are located at 0.009, 0.01, and 0.03 m from the origin, respectively. The number of control volumes is $(N_x, N_y) = (2401, 201)$ in Cartesian coordinates; and 1.8×10^6 computational particle parcels are used to represent particle clouds in the numerical simulation. The pressure of the unshocked area is 1×10^5 Pa and the incident Mach number is 1.2. We use 48 CPU cores for the computation due to the large parcel number.

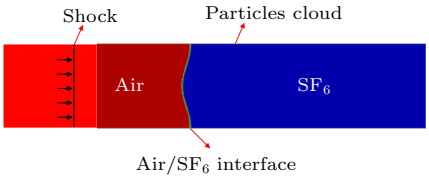

Fig. 1. The initial computational setup.

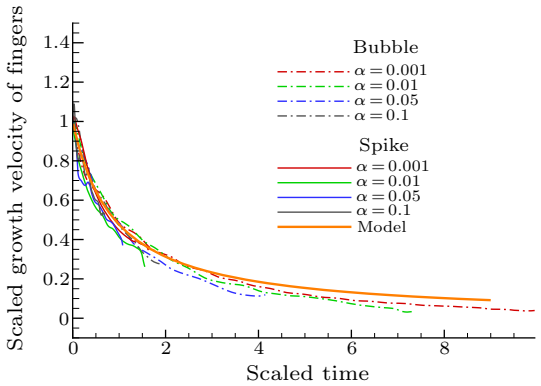

Fig. 2. Comparison between the model curve given by Eq. (18) and the scaled numerical finger growth velocity (solid lines for spike and dashed lines for bubbles) at different particle volume fractions.

The nonlinear finger growth in equilibrium flow (Eq. (14)), which depends on the particle volume fractions and particle density, is investigated firstly. The particle density is set as $50\,\mathrm{kg/m^3}$ and the diameter is set as $1\,\mu\mathrm{m}$. The particle volume fractions are 0.001, 0.01, 0.05, 0.1 in the different numerical cases. The response time of particle is estimated to be 10^{-7} s and the Stokes number is about 0.01. The scaled bubble growth velocity and scaled spike velocity can be obtained (Fig. 2). It can be seen that the profiles of the scaled finger growth velocities converge to the model curve. Due to the small Stokes number, the particles respond to fluid motion immediately. The interphase momentum exchange is rapid and the mechanical behavior of particles in equilibrium flow is similar to fluid. Thus, the effects of particles can be regarded as a change in the effective density of fluid.

In frozen flow, the nonlinear finger growth depends on the densities and volume fractions of the two fluids (Eq. (15)). Under our numerical conditions, the particles are uniformly distributed in the computational

domain, that is, $\alpha_{f,1} = \alpha_{f,2}$. Thus, the equivalent Atwood number reduces to the form in single-phase RMI. In order to satisfy the frozen flow's conditions, the density and drag term k should be small when setting numerical properties of particles. The particle density varies from 500 to 3000 kg/m^3. The diameter is set as 1 μm and the particle volume fraction is 0.05. The drag term is varied by changing the drag force coefficient in the Stokes law. In the different numerical cases, different coefficients are added on the drag force to ensure the Stokes numbers are the same. Here the Stokes number is about 1000.

As seen from Fig. 3, under the conditions of frozen flow, the evolution of the width of mixing zone in multiphase RMI is almost the same as that in single-phase RMI. For the reason why interphase momentum exchange is restrained in frozen flow, the motion of fluid phase is less affected. The profile of the width of mixing zone in frozen flow is almost the same as that in single-phase RMI. Therefore, the finger growth velocity should also be consistent with that in single-phase RMI. These results also verify the previous equivalent Atwood number (Eq. (15)), which means that particle density almost has no influence on the finger growth in frozen flow.

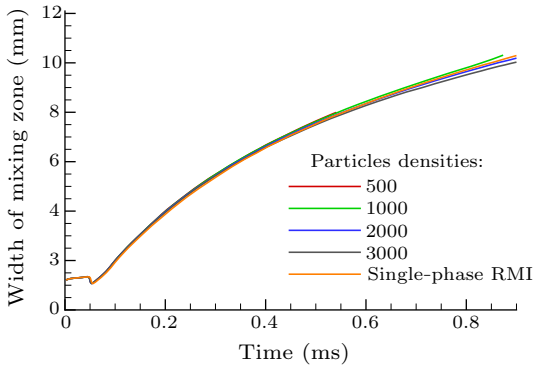

Fig. 3. Frozen flow: the evolution of the width of mixing zone at different particle densities.

When the Stokes number is moderate, in this case there exists gradual interphase momentum exchange. The velocity obtained by the particle phase will lead to the decrement of the energy of fluid motion. At different Stokes numbers, the interphase momentum changes will be different, resulting in the different interface motions. To get appropriate numerical conditions, the particle density is set as 2000 kg/m^3 and the particle volume fraction is 0.05. The diameter is also set as 1 μm. For the different numerical cases, the Stokes numbers are estimated to be 12, 27, 52 and 120, respectively.

Numerical results show that the width of mixing zone will be obviously different at different Stokes numbers (Fig. 4). With the increment of the Stokes number, the interphase momentum exchange will decrease apparently. Thus, energy for interface motion becomes large, leading to the increment of the width of the mixing zone. The reason why the equilibrium flow and frozen flow are two limit states in multiphase RMI is that the variation of the width of mixing zone ranges between the two model curves (dot-dashed line in Fig. 4(a)). The density contours at frozen flow and equilibrium flow are shown in Figs. 4(b) and 4(c). The interface growth at equilibrium flow is obviously restrained due to the effects of particles.

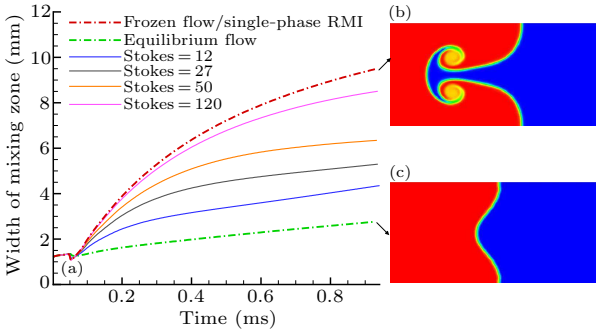

Fig. 4. (a) The evolution of the width of mixing zone at different Stokes numbers. Density contours at the end of simulation: (b) frozen flow and (c) equilibrium flow.

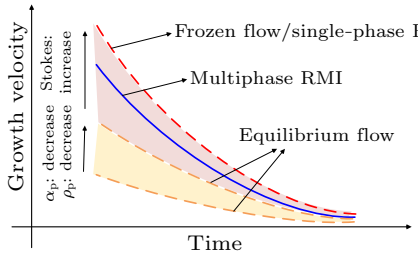

Fig. 5. Schematic illustrations of the nonlinear finger growth velocity in multiphase RMI.

Figure 5 shows schematic illustrations of the nonlinear finger growth velocity. The nonlinear finger growth velocity can be approximately determined in multiphase RMI. Firstly, we can obtain the accurate position of the curve of finger growth velocity at frozen flow, which only depends on the density ratio of fluids. Thus, the curves of finger growth velocity with different particle properties all converge to the model curve in single-phase RMI. At equilibrium flow, the curves of the finger growth velocity are associated with the particle volume fraction and the particle density. At various particle fractions and densities, the model curve for equilibrium flow will vary in the yellow region in Fig. 5. When the particle volume fraction and the particle density are fixed, the location of the curve of the nonlinear finger growth velocity (blue line in Fig. 5) is between the model curves of the frozen flow and equilibrium flow (red region in Fig. 5). The Stokes number will dominate the accurate location. With the increasing Stokes number, the effects of particles will be weakened and the profile of the finger growth velocity will get close to the model curve of the frozen flow/sing-phase RMI.

From these results, we can discuss the nonlinear finger growth in multiphase RMI in a simple way. The differences between the nonlinear growth in single-phase RMI and multiphase RMI are essentially attributed to the interphase momentum exchange. Three factors dominate the interface momen-

tum exchange: Stokes number, particle volume fraction and particle density. Under the condition of large Stokes number, low particle volume fraction and small particle density, the interphase momentum exchange will be restrained (frozen flow) and then the interface evolution in multiphase RMI will get close to that in single-phase RMI. In contrast, the interphase momentum exchange will be obvious (equilibrium flow), resulting in the apparent decrement of the nonlinear finger growth velocity in multiphase RMI. Viscosity, surface tension, elastic-plastic properties and magnetic field are all classical stabilization mechanisms in RM instability.[36–38] The effects of particles can be regarded as another stabilization mechanism, which slows down the growth of RMI.

In summary, the nonlinear finger growth of multiphase RMI in dilute gas-particle flow is systematically examined. A kind of widely accepted potential flow model is utilized to analyze the nonlinear finger growth in multiphase RMI. With this method, a universal model is proposed to quantitatively express the nonlinear finger growth velocity. In the limited cases, the analytical expressions for the model are derived. Furthermore, numerical simulations are conducted to investigate the multiphase RMI. Under the conditions of equilibrium flow and frozen flow, the numerical profile of the nonlinear finger growth velocity matches well with the model curve. When the Stokes number is moderate, the curve of finger growth velocity locates in the region between the two model curves.

References

[1] Zhou Y 2017 *Phys. Rep.* **720** 1
[2] Luo X S, Zhang F, Ding J C, Si T, Yang J M, Zhai Z G and Wen C Y 2018 *J. Fluid Mech.* **849** 231
[3] Zhang Q and Guo W X 2016 *J. Fluid Mech.* **786** 47
[4] Zhai Z G, Zhang F, Zhou Z B, Ding J C and Wen C Y 2019 *Sci. Chin.-Phys. Mech. Astron.* **62** 124712
[5] Li M and Ye W H 2019 *Chin. Phys. Lett.* **36** 025201
[6] Tian B L, Zhang X T, Qi J and Wang S H 2011 *Chin. Phys. Lett.* **28** 114701
[7] Gao F J, Zhang Y S, He Z W et al 2016 *Phys. Fluids* **28** 114101
[8] Raman K S, Smalyuk V A, Casey D T et al 2014 *Phys. Plasmas* **21** 072710
[9] Richtmyer R D 1960 *Commun. Pure Appl. Math.* **13** 297
[10] Meshkov E E 1972 *Fluid Dyn.* **4** 101
[11] Saffman P G 1962 *J. Fluid Mech.* **13** 120
[12] Ukai S, Balakrishnan K and Menon S 2010 *Phys. Fluids* **22** 104103
[13] Larsen M L, Shaw R A, Kostinski A B and Glienke S 2018 *Phys. Rev. Lett.* **121** 204501
[14] Mcfarland J A, Black W J, Dahal J and Morgan B E 2016 *Phys. Fluids* **28** 024105
[15] Parmar M, Haselbacher A and Balachandar S 2012 *J. Fluid Mech.* **699** 352
[16] Vorobieff P, Anderson M, Conroy J, White R, Truman C and Kumar S 2011 *Phys. Rev. Lett.* **106** 184503
[17] Lee C B, Peng H W, Yuan H J, Wu J Z, Zhou M D and Hussain F 2011 *J. Fluid Mech.* **677** 39
[18] Zhong H J, Lee C B, Su Z, Chen S Y, Zhou M D and Wu J Z 2013 *J. Fluid Mech.* **716** 228
[19] Xu T, Lien F S, Ji H and Zhang F 2013 *Shock Waves* **23** 619
[20] Boiko V M, Kiselev V P, Kiselev S P, Papyrin N A, Poplavsky S V and Fomin V M 1997 *Shock Waves* **7** 275
[21] Kandan K, Khaderi S N, Wadley H and Deshpande V S 2017 *J. Mech. Phys. Solids* **109** 217
[22] Zhang F, Frost D L, Thibault P A and Murray S B 2001 *Shock Waves* **10** 431
[23] Saito T 2002 *J. Comput. Phys.* **176** 129
[24] Saito T, Marumoto M and Takayama K 2003 *Shock Waves* **13** 299
[25] Saurel R, Chinnayya A and Carmouze Q 2017 *Phys. Fluids* **29** 063301
[26] Zhou Y 2017 *Phys. Rep.* **723** 1
[27] Meng B Q, Zeng J S, Tian B L, Li L, He Z W and Guo X H 2019 *Phys. Fluids* **31** 074102
[28] Nishihara K, Wouchuk J G, Matsuoka C, Ishizaki and Zhakhovsky V V 2010 *Philos. Trans. R. Soc. A* **368** 1769
[29] Balakrishnan K and Menon S 2011 *Laser Part. Beams* **29** 201
[30] Mikaelian K O 1998 *Phys. Rev. Lett.* **80** 508
[31] Mikaelian K O 2008 *Phys. Rev. E* **78** 015303
[32] Layzer D 1955 *Astrophys. J.* **122** 1
[33] Goncharov V N 2002 *Phys. Rev. Lett.* **88** 134502
[34] Zhang Q 1998 *Phys. Rev. Lett.* **81** 3391
[35] Snider D M, ORourke P J and Andrews M J 1998 *Int. J. Multiphase Flow* **24** 1359
[36] Guo H Y, Wang L F, Ye W H, Wu J F, Zhang W Y 2017 *Chin. Phys. Lett.* **34** 045201
[37] Yang X, Xiao D L, Ding N, Liu J 2017 *Chin. Phys. B* **26** 075202
[38] Mikaelian K O 1990 *Phys. Rev. A* **42** 7211